

On the highly inclined v_W leptokurtic asteroid families

V. Carruba,¹★ R. C. Domingos,^{1,2} S. Aljbaae¹ and M. Huaman¹

¹UNESP, Univ. Estadual Paulista, Grupo de dinâmica Orbital e Planetologia, Guaratinguetá 12516-410, SP, Brazil

²UNESP, Univ. Estadual Paulista, São João da Boa Vista 13874-149, SP, Brazil

Accepted 2016 August 11. Received 2016 August 11; in original form 2016 June 29

ABSTRACT

v_W leptokurtic asteroid families are families for which the distribution of the normal component of the terminal ejection velocity field v_W is characterized by a positive value of the γ_2 Pearson kurtosis, i.e. they have a distribution with a more concentrated peak and larger tails than the Gaussian one. Currently, eight families are known to have $\gamma_2(v_W) > 0.25$. Among these, three are highly inclined asteroid families, the Hansa, Barcelona, and Gallia families. As observed for the case of the Astrid family, the leptokurtic inclination distribution seems to be caused by the interaction of these families with node secular resonances. In particular, the Hansa and Gallia family are crossed by the $s - s_V$ resonance with Vesta, that significantly alters the inclination of some of their members. In this work we use the time evolution of $\gamma_2(v_W)$ for simulated families under the gravitational influence of all planets and the three most massive bodies in the main belt to assess the dynamical importance (or lack of) node secular resonances with Ceres, Vesta, and Pallas for the considered families, and to obtain independent constraints on the family ages. While secular resonances with massive bodies in the main belt do not significantly affect the dynamical evolution of the Barcelona family, they significantly increase the $\gamma_2(v_W)$ values of the simulated Hansa and Gallia families. Current values of the $\gamma_2(v_W)$ for the Gallia family are reached over the estimated family age only if secular resonances with Vesta are accounted for.

Key words: celestial mechanics – minor planets, asteroids: general.

1 INTRODUCTION

Of the three proper elements most commonly used to identify an asteroid family, the inclination is the one usually less affected by dynamical evolution. Secular resonances involving the precession frequency of the longitude of the node of an asteroid, like the linear secular resonance with Ceres $s - s_C$, can, however, change the inclination distribution of families crossed by this kind of resonances (Novaković et al. 2015). This is, for instance, the case of the Astrid family, that is characterized by a dispersion in inclination of its members at $a \simeq 2.764$ au much larger than that of members at other semi-major axis, giving this family a characteristics ‘crab-like’ appearance in the $(a, \sin(i))$ plane (Novakovic et al. 2016). Recently, Carruba (2016) used the time evolution of the Pearson kurtosis of the v_W component of terminal ejection velocities to set independent constraints on the Astrid family age and ejection velocity parameter V_{EJ} . Since v_W can be obtained by inverting the third Gauss’ equation and is mostly dependent on $\delta i = i - i_{ref}$, with i_{ref} the inclination of the barycentre of the family, families whose distribution in proper inclination is characterized by larger tails and more concentrated

peaks than that of a Gaussian distribution would have values of Pearson kurtosis $\gamma_2(v_W)$ larger than zero. By simulating fictitious families for different values of ejection velocities parameter V_{EJ} under the influence of the Yarkovsky non-gravitational force, and by observing when current values of $\gamma_2(v_W)$ were reached for the Astrid families it was possible to set independent constraints on the family age, V_{EJ} , and on key parameter determining the strength of the Yarkovsky force such as the mean density and surface thermal conductivity of family members.

Of the eight v_W leptokurtic families with $\gamma_2(v_W) > 0.25$, three are highly inclined families ($\sin(i) > 0.3$) in the central main belt: the Hansa, Barcelona, and Gallia families (Carruba & Nesvorný 2016). It has recently been suggested that these families could be interacting with node secular resonances with Vesta (Tsirvoulis & Novaković 2016). In this work we attempt to use the numerical tools developed for the Astrid family to (i) assess the importance (or lack of) of the $s - s_V$ secular resonance and of possible analogous resonances with Pallas, and (ii) set independent constraints on the three families ages. Overall, we found that the use of the $\gamma_2(v_W)$ could indeed provide valuable hints on the importance of secular resonances with massive bodies, and, more generally, on the whole dynamical evolution of $\gamma_2(v_W)$ leptokurtic asteroid families.

* E-mail: vcarruba@feg.unesp.br

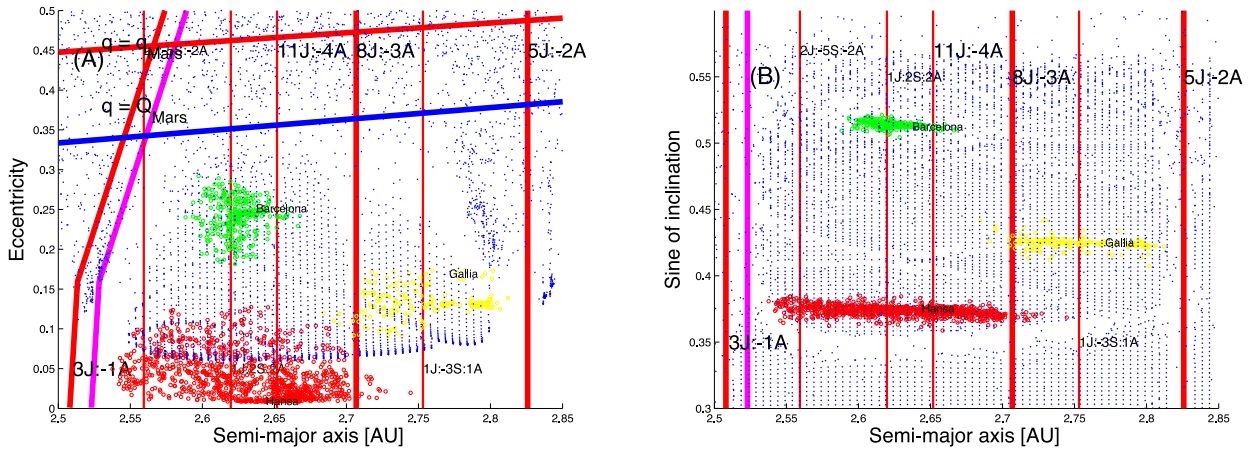


Figure 1. Dynamical maps in the proper (a, e) (panel A) and $(a, \sin(i))$ (panel B) domains. Vertical red lines display the location of the local mean-motion resonances. The magenta line identifies the width of the unstable chaotic layer near the 3J:-1A resonance, as identified in Morbidelli & Vokrouhlický (2003). The blue and red lines in the (a, e) plane identify the orbital location of asteroids whose pericentre q is equal to the apocentre and pericentre of Mars, respectively. The region depleted of test particles at $\sin(i) \simeq 0.35$ in the $(a, \sin(i))$ plane is associated with orbits in librating states of the ν_6 secular resonance. Other secular resonances appear as inclined bands of proper elements in the figure. Red, green and yellow filled dots display the orbital location of members of the Hansa, Barcelona, and Gallia dynamical families, respectively.

2 ASTEROID FAMILIES IDENTIFICATION

As a first step in our analysis of the ν_W leptokurtic highly inclined families, we start by identifying the Hansa, Barcelona and Gallia family in the space of proper elements, and by studying the local dynamics. For the first purpose, we use the data from Nesvorný, Brož & Carruba (2015), where these families were identified in the domain of proper $(a, e, \sin(i))$ using the hierarchical clustering method and cut-off velocities of 200 m s^{-1} for the Hansa and Gallia families and of 150 m s^{-1} for the Barcelona one. The groups so identified have 1094 members for the Hansa family, 182 for the Gallia group, and 306 for the Barcelona cluster. As also discussed in Carruba (2010), these three families have S-type taxonomies. Values of the mean geometric albedos for these three groups were 0.26 for Hansa, 0.17 for Gallia, and 0.25 for Barcelona, respectively (Nesvorný et al. 2015).

Carruba (2010) investigated in depth the local dynamical environment for these families. The author obtained dynamical maps in the domain of synthetic proper (a, e) , $(a, \sin(i))$, and $(e, \sin(i))$ domains. Highly inclined asteroid families in the central main belt are separated by the effect of the local secular dynamics. The strong $\nu_6 = g - g_6$ secular resonance acts as a dynamical barrier between highly inclined and low inclined asteroids. Of importance are also the other two main linear secular resonances, the $\nu_5 = g - g_5$ and the $\nu_{16} = s - s_6$, that, together with the local mean-motion resonances 3J:-1A, 8J:-3A, and 5J:-2A separate the regions into eight different stable islands. The region is also crossed by several interesting non-linear secular resonance, whose detailed identification and description can be found in Carruba (2010). Repeating the detailed dynamical analysis of Carruba (2010) is of course redundant and beyond the purposes of this paper. To allow the reader to have a visual understanding of the complex local dynamics, in this work we obtained dynamical maps of 7000 particles in the domains of synthetic proper (a, e) and $(a, \sin(i))$ with the same approach described in Carruba (2010). We refer the reader to that paper for a discussion of the methods and initial conditions used for obtaining these maps.

Fig. 1 displays our results in the (a, e) (panel A) and $(a, \sin(i))$ (panel B) planes. Vertical lines display the location of local

mean-motion resonances. Objects with eccentricities larger than 0.35 are Mars-crossers in this region of the main belt, and are lost on time-scales of $\simeq 1 \text{ Myr}$. The ν_6 secular resonance causes asteroids in librating states to increase their eccentricity to Mars-crossing levels, and to become unstable. The region associated with this resonance appears as a strip at $\sin(i) \simeq 0.35$ depleted of proper elements. Other secular resonances appear as inclined alignments of test particles. Apart from the ν_5 , important for its interaction with the Barcelona family (Froeschlé & Scholl 1989), and the ν_{16} linear secular resonances, important non-linear secular resonances in the region are the $\nu_6 - \nu_{16}$, $\nu_5 - \nu_{16}$, and $2\nu_6 - \nu_5 + \nu_{16}$ secular resonances. Hansa, Barcelona, and Gallia members are shown as red, green, and yellow filled dots, respectively.

Recently, Tsirvoulis & Novaković (2016) suggested that the linear secular resonances $\nu_{1V} = s - s_V$ with Vesta could have played a role in the dynamical evolution of the Barcelona and Hansa family. To further investigate this hypothesis, we obtained a dynamic map in the $(a, \sin(i))$ domain, (node secular resonances change values of asteroids proper inclinations) with the same initial conditions used before, but adding Ceres, Vesta, and Pallas as massive perturbers. Fig. 2 displays our results. Black circles identify objects whose proper frequency s is to within $\pm 0.2 \text{ arcsec yr}^{-1}$ from the value of Vesta, assumed equal to $-39.597 \text{ arcsec yr}^{-1}$. These are the objects most likely to be affected by this kind of resonant dynamics. Magenta circles do the same for objects whose s is $\pm 0.2 \text{ arcsec yr}^{-1}$ from $-46.393 \text{ arcsec yr}^{-1}$, the proper node precession frequency for Pallas. Pericentre resonances with Vesta were not found to be important for this region in Tsirvoulis & Novaković (2016), and the proper g frequency of Pallas is outside the range of values covered in this dynamical map. For these reasons, we did not further investigate the role of pericentre secular resonances with massive asteroids in this work. The ν_{1V} could in principle be affecting the dynamical evolution of the Hansa, Gallia, and, marginally, the Barcelona families. The ν_{1P} resonance, however, does not seem to interact with any of these families, and could play a minor role just for the case of the Hansa family. We will further investigate the role played by those resonances in the next sections.

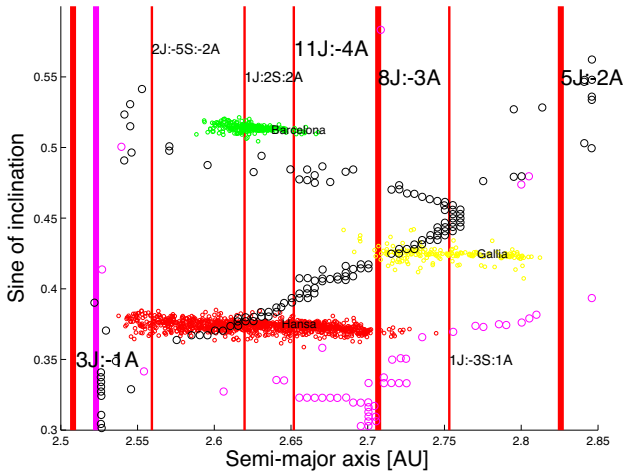


Figure 2. A dynamical map in the $(a, \sin(i))$ domain for the same region displayed in Fig. 1, but obtained also considering the effect of Ceres, Vesta and Pallas as massive perturbers. Black circles display the location of likely resonators in the ν_{1V} secular resonance, while magenta circles are associated with likely resonators of the ν_{1P} resonance. Other symbols are the same as in Fig. 1, panel B.

Having briefly revised the local dynamics, we then turn our attention to the taxonomic properties of the three studied families. Taxonomic properties and geometric albedo values of all highly inclined families in the central main belt were studied in Carruba (2010) in some detail. The three families all belong to the S-type taxonomic class. There are 94 objects with photometric data compatible with a S-type composition in the Sloan Digital Sky Survey-Moving Object Catalog data, fourth release (SDSS-MOC4 hereafter; Ivezić et al. 2001) in this region. 470 objects have geometric albedo and absolute magnitude information in the *WISE* and NEOWISE data base (Masiero et al. 2012).

Fig. 3 display asteroids whose SDSS-MOC4 photometric data is compatible with an S-type composition, according to the classifications method of DeMeo & Carry (2013) (panel A). Panel B displays objects whose *WISE* geometric albedo p_V has values compatible with an S-complex taxonomy, (i.e. $0.12 < p_V < 0.30$; Masiero et al. 2012). As can be seen from the figure, most of the objects with photometric and albedo S-type compatible data are indeed

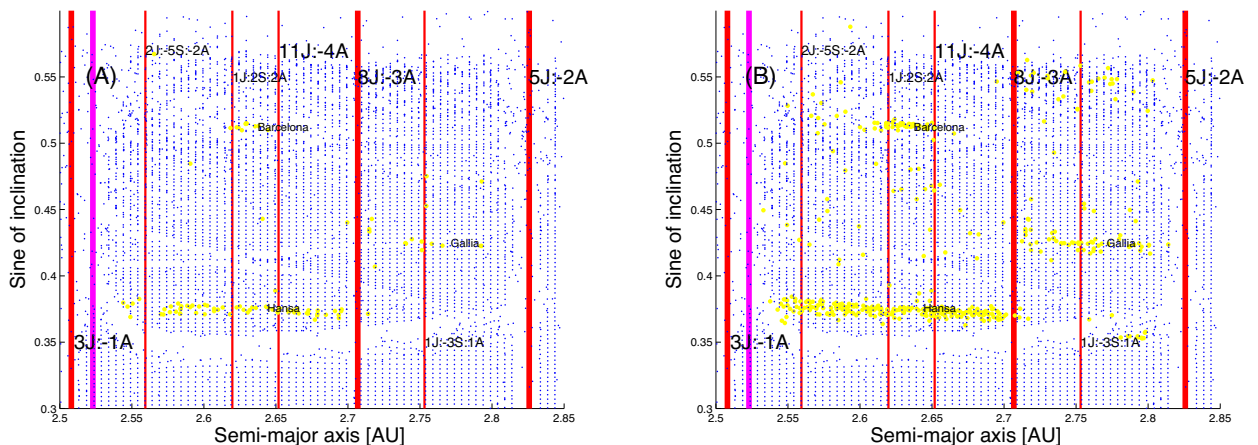


Figure 3. Panel A: yellow filled dots identify objects whose SDSS-MOC4 photometric data is compatible with an S-type composition. Panel B: objects with *WISE* albedo p_V in the range from 0.15 to 0.30. Other symbols are the same as in Fig. 1, panel B.

Table 1. Values of $\gamma_2(v_W)$ of the whole family (third column), the $2.0 < D < 4.0$ km (D_3) members (fourth column), the p coefficient of the jbest (fifth column), and estimated family age with its error (sixth column) from Nesvorný et al. (2015) for the Hansa, Barcelona, and Gallia families.

FIN	Family name	$\gamma_2(v_W)$ All	$\gamma_2(v_W)$ D_3	p_{jbest} (per cent)	Age [Myr]
803	480 Hansa	0.81	1.17	0.1	2430 ± 600
805	945 Barcelona	1.48	1.32	0.5	250 ± 10
802	148 Gallia	2.02	3.39	0.1	650 ± 60

associated with the three studied families. Using the SDSS-MOC4 data, we tried to obtain haloes for the three families with the method discussed in Carruba, Nesvorný & Aljbae (2016) for the Koronis family. In this method, asteroids with SDSS-MOC4 data are considered to be members of the halo of the family if their values of proper eccentricity and inclination are in a range from the centre of dynamical family to within four standard deviations of e and $\sin(i)$ of the distribution observed for the HCM family. We applied this method for the three studied families, but, unfortunately, we are limited by small number statistics for the cases of the Gallia and Barcelona families, that have haloes of less than 10 members. The Hansa family has a halo of 63 members, but its distribution in proper inclination is comparable to that of the HCM family. For the purpose of studying the Kurtosis of the v_W component of terminal ejection velocities, we are therefore left using standard HCM data alone. The apparent lack of significant haloes for these three families may be caused by the fact that these groups are contained in stable islands surrounded by unstable regions, which limits the number of long-term surviving outlying asteroids.

Carruba & Nesvorný (2016) studied the shape of the v_W component of the ejection velocity field of these three families, that are among the most leptokurtic among the studied group. For the sake of the reader not familiar with that work, we summarize in Table 1 the result of that study. The first two columns report the Family Identification Number (FIN), as defined in Nesvorný et al. (2015), and the family identification and name. The third and fourth columns report the values of $\gamma_2(v_W)$ for the whole family and for the D_3 population with $2.5 < D < 3.5$ km, respectively. The fifth column displays the result of the Jarque–Bera statistical test of the distribution being compatible with a Gaussian distribution (0.5 per cent being the null probability level of the two distributions being

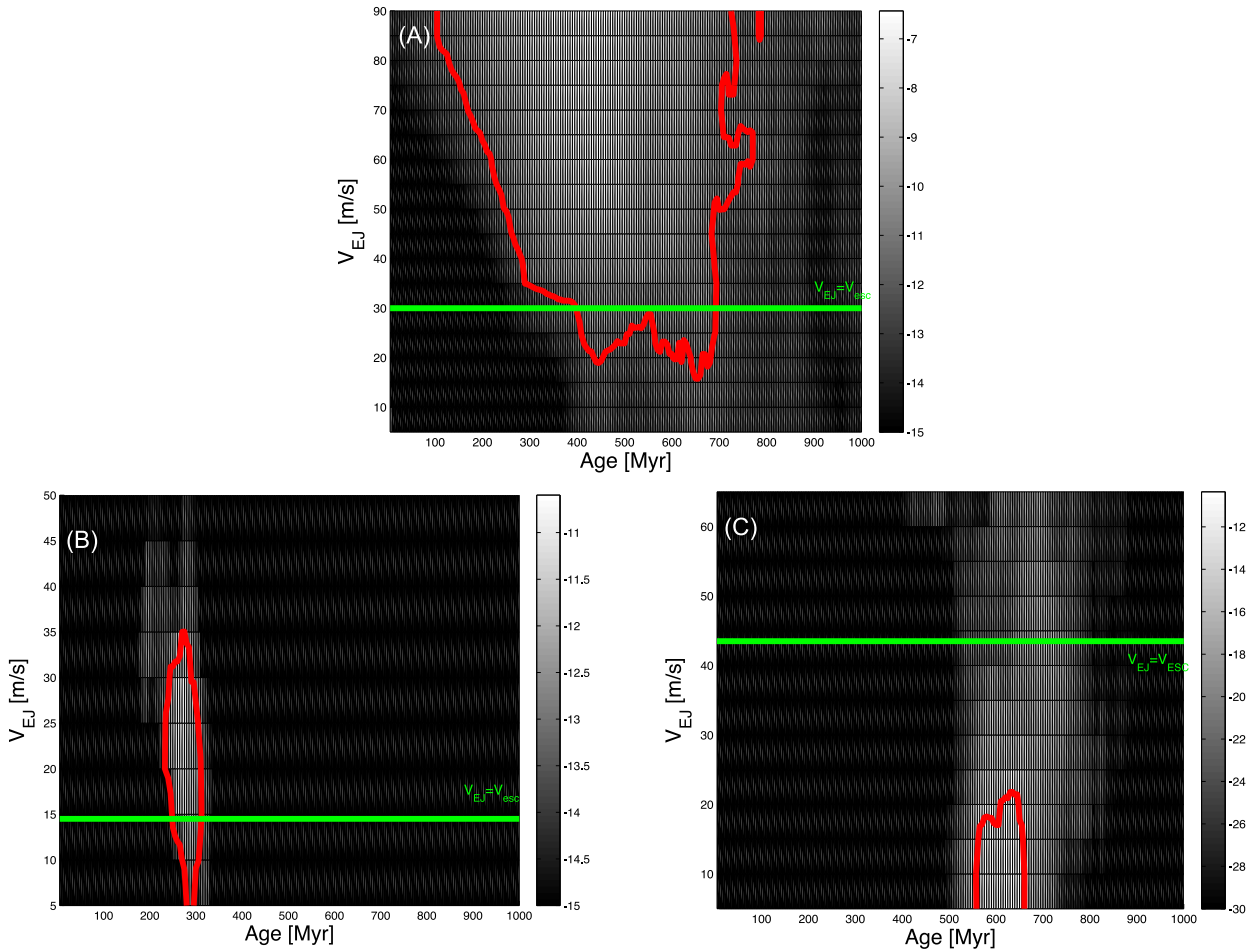


Figure 4. Target function $\psi_{\Delta C}$ values in (Age, V_{EJ}) plane for the Hansa (panel A), Barcelona (panel B), and Gallia families (panel C). The horizontal green lines display the value of the estimated escape velocities V_{ESC} from the parent body. The red lines display the contour level of $\psi_{\Delta C}$ associated with a 1σ probability that the simulated and real distribution were compatible.

compatible). Finally, the sixth column reports the estimated age and its error from Nesvorný et al. (2015), computed using the procedure discussed in Carruba & Nesvorný (2016), section 4. The time evolution of the v_W component of simulated families will be discussed later on in this paper.

3 CHRONOLOGY

There is a considerable range of possible values for the age of the Hansa family in the literature. Carruba (2010), using the method of Yarkovsky isolines, provided an upper limit for the family age of 1600 Myr old (see also Brož et al. (2013)). The estimate from Nesvorný et al. (2015) was of 2430 ± 60 Myr, while Spoto, Milani & Knežević (2015), using a V-shape criteria, assessed the family age to be in the range 420–1170 Myr. The age of the Barcelona family was estimated by Carruba (2010) (see also Brož et al. 2013) to have an upper limit of 350 Myr and to be in the range of 250 ± 10 Myr by Nesvorný et al. (2015). The Gallia family had an upper limit of 450 Myr in Carruba (2010) (see also Brož et al. 2013) and an age estimate of 650 ± 60 Myr in Nesvorný et al. (2015). No estimates for the ages of the Barcelona and Gallia family was provided in Spoto et al. (2015).

Here we try to obtain a new estimate of the families ages using the approach described in Carruba et al. (2015), that uses a Monte

Carlo method (Vokrouhlický et al. 2006a,b,c; Novaković, Tsiganis & Knežević 2010). The method has been described in several previous papers, so here we just shortly summarized the approach. Interested readers can find more details in Carruba et al. (2015). Basically, fictitious families with different values of V_{EJ} , a parameter describing the shape of the family ejection velocity field, are generated and then evolved under the influence of the Yarkovsky and YORP effects, and taking into account that solar luminosity was less intense in the past. The obtained distribution of a C parameter, that depends on the asteroids semi-major axis and absolute magnitude, is then compared to the one observed for the real asteroid family, and a χ^2 -like variable $\psi_{\Delta C}$ is then used to evaluate which fictitious family best approximate the C distribution of the real asteroid group. We applied this method to the Hansa, Barcelona, and Gallia families, and Fig. 4 displays our results in the (Age, V_{EJ}) plane. The radius of the family parent body, as estimated from Nesvorný et al. (2015), and the escape velocity V_{ESC} are reported in Table 2. Since Carruba & Nesvorný (2016) showed that most asteroid families have values of V_{EJ} not greater than $1.5 V_{ESC}$, we considered values of V_{EJ} going from 0 up to 90 m s^{-1} , i.e. equal to 1.5 the estimated escape velocity ($\approx 60 \text{ m s}^{-1}$) from the Hansa parent body, the body with the largest escape velocity among the families here studied.

At a 1σ level of probability of the simulated family distribution being compatible with the real one (red curve in Fig. 4, associated

Table 2. Number of family members (N_{mem}), mean geometric albedo (p_V), estimated radius of the parent body (R_{PB}), escape velocities (V_{ESC}), estimated V_{EJ} , and ages T for the Hansa, Barcelona, and Gallia families.

Family	N_{mem}	p_V	R_{PB} (km)	V_{ESC} (m s $^{-1}$)	V_{EJ} (m s $^{-1}$)	T (Myr)
Hansa	1094	0.26	28.0	30.0	80^{+10}_{-65}	460^{+280}_{-360}
Barcelona	306	0.25	13.5	14.5	15^{+20}_{-15}	265^{+45}_{-35}
Gallia	182	0.17	40.5	43.4	5^{+17}_{-5}	630^{+30}_{-70}

$\psi_{\Delta C} = 10.73$ and 12 degree of freedoms for our distribution) we found that $T = 460^{+280}_{-360}$ Myr, and $V_{\text{EJ}} = 80^{+10}_{-65}$ m s $^{-1}$ for the Hansa family, $T = 265^{+45}_{-35}$ Myr, and $V_{\text{EJ}} = 15^{+20}_{-15}$ m s $^{-1}$ for the Barcelona family, and $T = 630^{+30}_{-70}$ Myr, and $V_{\text{EJ}} = 5^{+17}_{-5}$ m s $^{-1}$ for the Gallia one. Again, our results are summarized in Table 2.

4 DYNAMICAL EVOLUTION OF v_W LEPTOKURTIC FAMILIES

The time evolution of the kurtosis of the v_W component of the ejection velocity field was recently used by Carruba (2016) to set constraints on the age and acceptable values of key parameters describing the Yarkovsky force, such as the surface thermal conductivity and asteroid density of the Astrid asteroid family. Here we use the same approach to investigate the dynamics of the three v_W leptokurtic highly inclined families. The setup of the simulations was discussed in Carruba (2016), interested readers could find more details in that paper. Basically, we simulated fictitious families with their currently observed size–frequency distribution, values of the parameters affecting the strength of the Yarkovsky force typical of S-type asteroids according to Brož et al. (2013), i.e. bulk and surface density, ρ_{bulk} and ρ_{surf} , equal to 1500 and 2500 kg m $^{-3}$, respectively, thermal conductivity $K = 0.001$ W m $^{-1}$ K $^{-1}$, thermal capacity equal to $C_{\text{th}} = 680$ J kg $^{-1}$ K $^{-1}$, Bond albedo $A_{\text{Bond}} = 0.1$,¹ and infrared emissivity $\epsilon = 0.9$. We also generated fictitious families with the optimal values of the ejection parameter V_{EJ} found in Section 3, for the three families Particles were integrated with *SWIFT_RMVS*, the symplectic integrator developed by Brož (1999) that simulates the diurnal and seasonal versions of the Yarkovsky effect, over 1000 Myr for the Hansa family, 600 Myr for the Barcelona group, and 800 Myr for the Gallia cluster, a time long enough to cover the putative estimated ages of these families. Two sets of simulations were performed. In the first we accounted for all planets from Mercury to Neptune, while in the second we also include Ceres, Vesta, and Pallas as massive bodies. Once proper elements were obtained, then values of v_W were computed by inverting the third Gauss equation (Murray & Dermott 1999):

$$\delta i = \frac{(1 - e^2)^{1/2}}{na} \frac{\cos(\omega + f)}{1 + e \cos(f)} \delta v_W. \quad (1)$$

where $\delta i = i - i_{\text{ref}}$, with i_{ref} the inclination of the barycentre of the family, and f and $\omega + f$ assumed equal to 30° and 50°5, respectively.

¹ Since the mean geometric albedo value of the Gallia family is lower than that of the other two families, and since this could imply a lower value of the Bond albedo, we also performed two additional sets of simulations for this family with a value of Bond albedo $A_{\text{Bond}} = 0.07$. The overall trend of the results of this simulations was compatible with that of the standard simulations with $A_{\text{Bond}} = 0.1$.

As discussed in Carruba (2016), the shape of the v_W distribution (and therefore its kurtosis), are not strongly dependent on the values of f and $\omega + f$.

Fig. 5 displays our results for the set of six simulations. Since the value of $\gamma_2(v_W)$ increased significantly when isolated objects drift beyond 4σ values in $\sin(i)$ from the centre of the family, as in Carruba & Nesvorný (2016) we eliminated from our computations of this parameters objects with inclination beyond that range. In particular, this meant considering asteroids with inclination between 21°6 and 22°4 for the Hansa family, between 27°8 and 29°1 for the Barcelona family, and between 24°0 and 26°2 for the Gallia family. Results for the Hansa family without the effect of massive asteroids show that values of $\gamma_2(v_W)$ are compatible with the current one for times larger than 200 Myr, which sets a lower limit on the family age. Including the massive asteroids only slightly alters this scenario, which suggest that the effect of resonances with Vesta for the Hansa family should be minor, when compared with other local resonances able to affect the inclination in the region. Spikes in the time behaviour of $\gamma_2(v_W)$ are associated with isolated asteroids whose inclination temporarily approached values of $\sin(i)$ close to the limits considered in our analysis. Of course, changing the allowed limits of $\sin(i)$ could modify the length and the shape of the isolated spikes observed in Fig. 5. Since our goal in this paper is, however, to assess the importance of different dynamical models and since we are using the same limits for the model with and without massive asteroids, we believe that our approach should be reasonable.

Concerning the Barcelona family, resonances with massive asteroids are not important for this family, as shown in Fig. 5, panels C and D. Results are essentially identical with and without massive asteroids, as expected from the results of Section 2, that showed that the Barcelona family is not actually crossed by the v_{1V} resonance, or other resonances with massive bodies. This negative result, however, confirm the usefulness of the $\gamma_2(v_W)$ as a tool to investigate the long-term behaviour of secular dynamics. As observed for the Astrid family (Carruba 2016), commonly used values of the key parameters density and thermal conductivity for S-type families are not able to produce the currently observed value of $\gamma_2(v_W)$ over the estimated age of the family. This could be either caused by (i) the fact that the mean values of density and thermal conductivity for members of the Barcelona family could be higher, or (ii) that the actual age of this family could be younger than what obtained from estimates from the Monte Carlo method of Section 3. An analysis of the full dependence of the $\gamma_2(v_W)$ time behaviour on values of density and thermal conductivity for the Barcelona family performed in the same way as recently done for the Astrid cluster seems to be outside the goals of this paper, that focused on studying the effectiveness of the use of $\gamma_2(v_W)$ as a tool to investigate the long-term effect of secular dynamics. But it certainly remains an interesting topic for future research.

Finally, the case of the Gallia family is of particular interest. If we do not consider the effect of secular resonances with Vesta, the simulated $\gamma_2(v_W)$ does not reach current values over the estimated age of the family. But there is an excellent agreement if we include secular perturbations from massive asteroids, as shown in Fig. 5, panel F. The larger values of $\gamma_2(v_W)$ obtained when massive asteroids are considered and the agreement with estimates of the Gallia family age obtained with independent methods represent, in our opinion, some of the newest and most interesting results of this work.

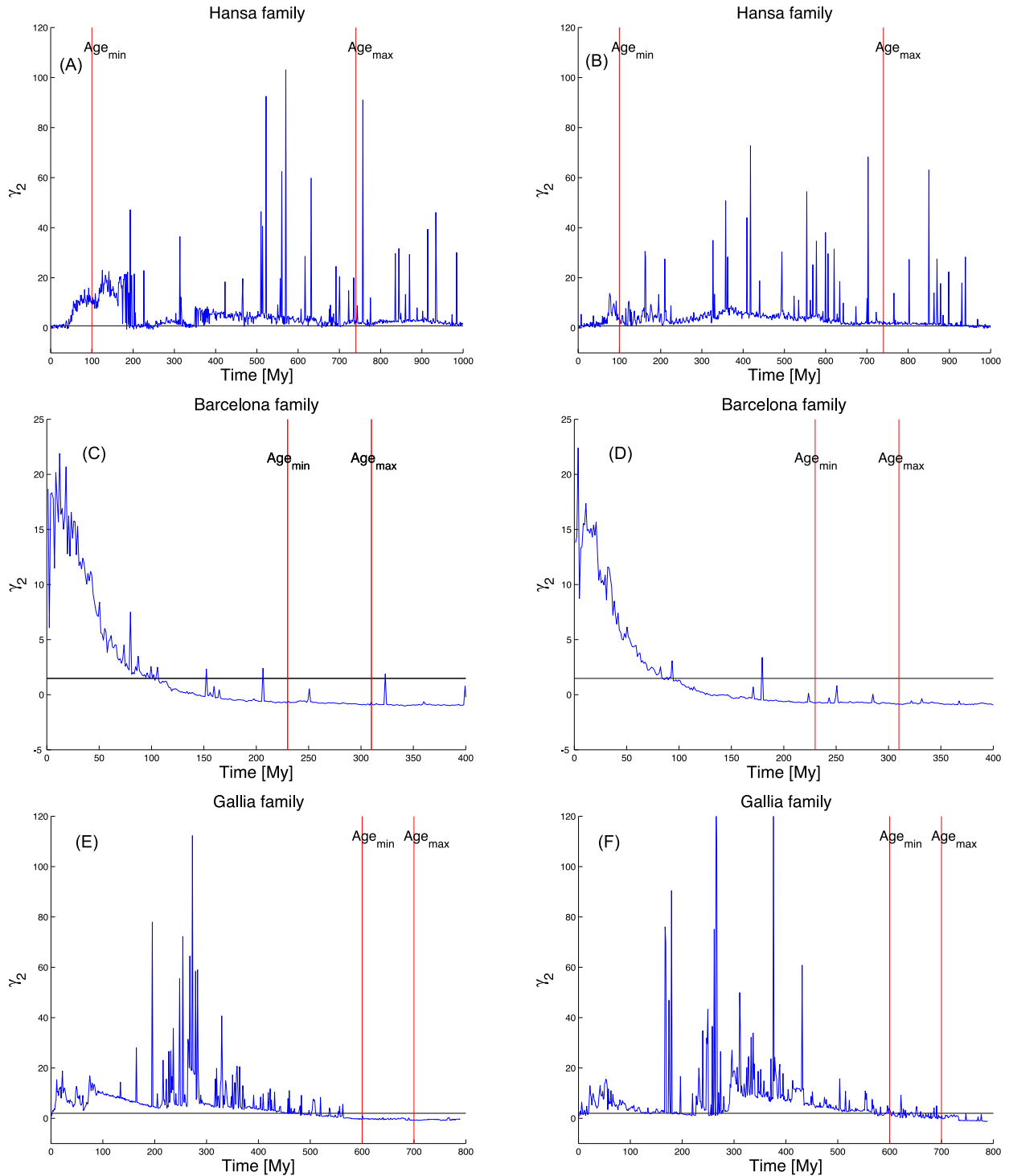


Figure 5. Time dependence of the kurtosis of the v_W component of the ejection velocity field ($\gamma_2(v_W)$) for the simulated Hansa, Barcelona, and Gallia families (panels A, C, and E, respectively). Panels B, D, and E display the same, but for the simulation where Ceres, Pallas, and Vesta were considered as massive perturbers. The horizontal black line display the current values of the families $\gamma_2(v_W)$, while the vertical red lines show the estimated range of possible ages.

5 CONCLUSIONS

Our results could be summarized as it follows.

(i) We identified the Hansa, Barcelona, and Gallia families in the domain of proper elements, obtained dynamical maps in the domains of proper (a, e) and $(a, \sin(i))$, and mapped the location in the $(a, \sin(i))$ of the three node resonance with Ceres, Vesta,

and Pallas. The Hansa and Gallia families are crossed by the $v_{1V} = s - s_V$ secular resonances. All families are S-complex group, all characterized by relatively large values of $\gamma_2(v_W)$.

(ii) We obtained age and terminal ejection velocities estimates for the three families using a Monte Carlo method to simulate the Yarkovsky and stochastic YORP evolution in proper a of family members. At 1σ confidence level we found that $T = 460^{+280}_{-360}$ Myr,

and $V_{\text{EJ}} = 80^{+10}_{-65}$ m s⁻¹ for the Hansa family, $T = 265^{+45}_{-35}$ Myr, and $V_{\text{EJ}} = 15^{+20}_{-15}$ m s⁻¹ for the Barcelona family, and $T = 630^{+30}_{-70}$ Myr, and $V_{\text{EJ}} = 5^{+15}_{-5}$ m s⁻¹ for the Gallia one. Our results are summarized in Table 2.

(iii) Simulated the dynamical evolution of fictitious families with values of the ejection velocity parameters V_{EJ} obtained from our previous analysis under the gravitational influence of all planets, the Yarkovsky force, and the effect of Ceres, Vesta, and Pallas. The $\gamma_2(v_W)$ parameter was computed as a function of time for all simulated family members, and we monitored when its value was comparable to the currently observed ones. The Gallia and, in a less measure, the Hansa families were significantly affected by secular resonances with Vesta. Current values of $\gamma_2(v_W)$ for the Gallia family could only be reached over the estimated family age if secular resonances with Vesta were accounted for. Conversely, secular resonances with main belt massive bodies play no significant role in the evolution of the Barcelona family. Independent constraints on the family age can be set by the time behaviour of the $\gamma_2(v_W)$ parameter.

Overall, we found that the $\gamma_2(v_W)$ parameter could be an invaluable tool for providing hints about the relative importance of secular dynamics, and to set constraints on the ages, ejection velocity fields, and key parameters influencing the Yarkovsky force, such as the mean density and surface conductivity of v_W leptokurtic families, and could be in principle applied to other similar families identified in Carruba & Nesvorný (2016).

ACKNOWLEDGEMENTS

We are grateful to the reviewer of this paper, Dr Bojan Novaković, for comments and suggestions that greatly improved the quality of this paper. We would like to thank the São Paulo State Science Foundation (FAPESP) that supported this work via the grant 2016/04476-8, and the Brazilian National Research Council (CNPq, grant 305453/2011-4). This publication makes use of data products from the *Wide-field Infrared Survey Explorer (WISE)* and NEOWISE, which are a joint project of the University of

California, Los Angeles, and the Jet Propulsion Laboratory/California Institute of Technology, funded by the National Aeronautics and Space Administration.

REFERENCES

- Brož M., 1999. Thesis, Charles Univ.
 Brož M., Morbidelli A., Bottke W. F., Rozenhal J., Vokrouhlický D., Nesvorný D., 2013, *A&A*, 551, A117
 Carruba V., 2010, *MNRAS*, 408, 580
 Carruba V., 2016, *MNRAS*, 461, 1605
 Carruba V., Nesvorný D., 2016, *MNRAS*, 457, 1332
 Carruba V., Nesvorný D., Aljbaae S., Domingos R. C., Huaman M. E., 2015, *MNRAS*, 451, 4763
 Carruba V., Nesvorný D., Aljbaae S., 2016, *Icarus*, 271, 57
 DeMeo F., Carry B., 2013, *Icarus*, 226, 723
 Froeschlé Ch., Scholl H., 1989, *Celest. Mech. Dyn. Astron.*, 46, 231
 Ivezić Ž. et al., 2001, *AJ*, 122, 2749
 Masiero J. R., Mainzer A. K., Grav T., Bauer J. M., Jedicke R., 2012, *ApJ*, 759, 14
 Morbidelli A., Vokrouhlický D., 2003, *Icarus*, 163, 120
 Murray C. D., Dermott S. F., 1999, *Solar System Dynamics*. Cambridge Univ. Press, Cambridge
 Nesvorný D., Brož M., Carruba V., 2015, In Michel P., DeMeo F. E., Bottke W., eds, *Asteroid IV*. Univ. Arizona Press and LPI, Tucson, AZ, p. 297
 Novaković B., Tsiganis K., Knežević Z., 2010, *MNRAS*, 402, 1263
 Novaković B., Maurel C., Tsirvoulis G., Knežević Z., 2015, *ApJ*, 807, L5
 Novaković B., Tsirvoulis G., Maro S., Djosovic V., Maurel C., 2016, in Proc. IAU Symp. 318, *Asteroids: New Observations, New Models*, p. 46
 Spoto F., Milani A., Knežević Z., 2015, *Icarus*, 257, 275
 Tsirvoulis G., Novaković B., 2016, preprint ([arXiv:1607.02035](https://arxiv.org/abs/1607.02035))
 Vokrouhlický D., Brož M., Morbidelli A., Bottke W. F., Nesvorný D., Lazzaro D., Rivkin A. S., 2006a, *Icarus*, 182, 92
 Vokrouhlický D., Brož M., Bottke W. F., Nesvorný D., Morbidelli A., 2006b, *Icarus*, 182, 118
 Vokrouhlický D., Brož M., Bottke W. F., Nesvorný D., Morbidelli A., 2006c, *Icarus*, 183, 349

This paper has been typeset from a $\text{\TeX}/\text{\LaTeX}$ file prepared by the author.